Revised Version Ms. #7764

Are the Thermodynamic Properties of Natural and Synthetic Mg_2SiO_4-Fe_2SiO_4 Olivines the Same?

Charles A. Geiger*, Noreen M. Vielreicher and Edgar Dachs

Department of Chemistry and Physics of Materials
Section Materials Science and Mineralogy
Salzburg University
Jakob Haringer Strasse 2a
A-5020 Salzburg, Austria

*Corresponding author
Tel. (0431) 662-8044-6226
E-mail: ca.geiger@sbg.ac.at

Submitted to American Mineralogist – Oct. 2, 2020

Short Title: Thermodynamics of Natural and Synthetic Olivines

ABSTRACT

It is not known if the thermodynamic behavior of some rock-forming minerals and their synthetic analogues are quantitatively the same. Olivine is an important rock-forming substitutional solid solution consisting of the two end-members forsterite, Mg_2SiO_4, and fayalite, Fe_2SiO_4. We undertook first C_p measurements on two natural olivines between 2 and 300 K; nearly end-member fayalite and a forsterite-rich crystal $Fo_{0.904}Fa_{0.096}$. Their $C_p(T)$ behavior is compared to that of synthetic crystals of similar composition, as found in the literature. The two natural olivines are characterized by X-ray powder diffraction and ^{57}Fe Mössbauer spectroscopy. The X-ray results show that the crystals are well crystalline. The Mössbauer hyperfine parameters, obtained from a fit with two Fe^{2+} quadrupole split doublets, are similar to published values measured on synthetic olivines. There are slight differences in the absorption line widths (i.e., FWHM) between the natural and synthetic crystals. C_p (2 to 300 K) is measured by relaxation calorimetry. The C_p results of the natural nearly end-member fayalite and published values for two different synthetic Fa_{100} samples are in excellent agreement. Even C_p resulting from a Schottky anomaly and a paramagnetic-antiferromagnetic phase transition with both arising from Fe^{2+} are similar. There are slight differences in the Néel temperature between the natural, 63 K, and synthetic, ~65 K, fayalites. This is probably related to the presence of additional minor elements (e.g., Mn^{2+}) in the natural crystal. The $S°$ value is 151.6 ± 1.1 J/mol·K. C_p behavior of the natural forsterite, $Fo_{0.904}Fa_{0.096}$, and a synthetic $Fo_{90}Fa_{10}$ olivine are in excellent agreement between about 7 and 300 K. The only difference lies at $T < 7$ K, as the former does not show Debye T^3 behavior, but, instead, a plateauing of C_p values. The $S°$ value for the natural forsterite is 99.1 ± 0.7 J/mol·K.

Key Words: Thermodynamics, Calorimetry, Heat Capacity, Entropy, Olivine, ^{57}Fe Mössbauer Spectroscopy

INTRODUCTION

The database of thermodynamic properties of rock-forming minerals is large. However, in spite of the great amount of research that has been done, there are still various outstanding issues. One important issue concerns the thermodynamic behavior of minerals and their synthetic analogues. This is critical because there is an underlying assumption in the community that there are no or negligible energetic differences between synthetic and natural crystals. The compilation of calorimetrically determined properties of Robie and Hemingway (1995) contains, for example, results obtained on both natural and synthetic phases. Internally consistent thermodynamic databases use phase-equilibrium and calorimetric results, obtained on the two types of crystals as well, to derive "best-fit" values of different thermodynamic functions. There could be, though, quantitative differences in the thermodynamic properties for some minerals.

Helgeson et al. (1978) wrote in their "Summary and Critique of the Thermodynamic Properties of Rock-Forming Minerals" that the two types of phases could behave differently. However, since then, little research has addressed this issue. Geiger and Dachs (2018) did analyze the standard third-law entropy, $S°$, value of various "end-member" silicate garnets both synthetic and natural. In two cases (i.e., almandine and andradite), there was no marked difference between synthetic and natural crystals in terms of calorimetric heat-capacity measurements, C_p(0-300 K), which were used to obtain $S°$. They noted, though, that older calorimetric C_p(0-300 K) measurements may not have been fully quantitative in some cases because of different technical issues. On the other hand, in the case of grossular, $Ca_3Al_2Si_3O_{12}$, where multiple calorimetric studies on various natural and synthetic crystals have been made and in several independent laboratories, there are small but measurable variations in $C_p(T)$ behavior and $S°$ values (Dachs et al. 2012; Geiger and Dachs 2018).

Constant pressure heat capacity, $C_p(T)$, is an essential thermodynamic function of any crystalline substance, especially at low temperatures (Westrum 1962)[1]. It can be measured directly via calorimetry. It is defined as

$$C_p = \left(\frac{dH}{dT}\right)_P \quad (1),$$

where H is the enthalpy. From it, $S°$ can be calculated via:

$$S^o - S^{T=0K} = \int_0^{298.15} \frac{C_P}{T} dT \quad (2),$$

assuming $S^{T=0K} = 0$. $S°$ can also be considered the calorimetric entropy.

Olivine is an important substitutional solid-solution silicate consisting of the two end-members forsterite, Mg_2SiO_4, and fayalite, Fe_2SiO_4. It occurs in meteorites, asteroids and in solid planets and their moons, and it is the most abundant phase in Earth's upper mantle. A precise knowledge of olivine's thermodynamic properties is crucial for undertaking a variety of mineralogical, petrological, geochemical and geophysical investigations. One area of current geochemical and metamorphic research is focusing on mineral carbonation and serpentinization of peridotite (Keleman et al. 2011). Here, relatively low-temperature olivine-bearing reactions are of importance. Olivine's thermodynamic behavior is complex and involves the atomic mixing of Fe^{2+} and Mg over two crystallographically independent octahedrally coordinated sites M1 and M2. Their mixing is temperature and composition dependent. Moreover, intermediate Fe^{2+}-bearing olivines show a low-temperature magnetic phase transition and a Schottky anomaly. Robie et al. (1982a, b) measured the low-temperature C_p (5-300 K) of synthetic end-member forsterite and fayalite, respectively, using adiabatic calorimetry. Dachs et al. (2007) also measured both end-members and, in addition, a number of synthetic intermediate-composition,

[1] "The solid state researcher so often has occasion to acknowledge the extraordinary wealth of information that can be obtained about substances from low-temperature heat capacity determinations that one is tempted to attribute to such measurements a more fundamental significance than to any other unique method of investigation."

$(Mg_{1-x},Fe^{2+}_x)_2SiO_4$, crystals using relaxation calorimetry. As best we know, no C_p(0-300 K) measurements have been made on natural olivine.

In light of this, this study presents first low-temperature C_p measurements of two different composition natural olivines. The results are compared to those obtained on synthetic crystals and an analysis of the thermodynamic behavior is made and conclusions drawn.

METHODS

Samples

Two natural olivine samples with different compositions, including a nearly end-member fayalite and a forsterite ($Fo_{0.904}Fa_{0.096}$), were selected for study. They are described in Table 1. Their compositions are given in Table 2. A fayalite-rich rock chip (Rockport, MA) roughly two cm size was crushed to a sand size and clear olivine grains were carefully hand-picked under a binocular to obtain a clean separate. The forsterite-rich olivine (Pyaung-gaung Mine, Myanmar) was prepared as a doubly polished platelet, about 3.3 x 4.3 x 1.0 mm, as taken from a larger single crystal.

X-ray powder diffraction, ^{57}Fe Mössbauer spectroscopy, and low-temperature C_p measurements

Sample purity was checked via x-ray powder diffraction (XRPD) using a Bruker D8 Advance with DaVinci-Design diffractometer (Bruker AXS, Karlsruhe, Germany). Splits from both samples were ground, mounted on a single-crystal silicon holder and measured using Cu Kα radiation (40 kV, 40 mA) in continuous mode between $5° \leq 2\theta \leq 95°$ with a step size of 0.015° and 0.15 sec/step. The diffractometer has a Bragg-Brentano beam geometry with a fixed 0.3° divergence slit, primary and secondary side 2.5° Soller slits, a 4.0° antiscatter slit and an energy dispersive Lynxeye detector (opening angle 2.934°). Silicon powder NBS SRM 640b was

used as an external calibration standard. Data were plotted using DIFFRAC.EVA (Version 5.0.0.22, 2019, Bruker AXS Inc., WI, USA).

The experimental ^{57}Fe Mössbauer spectroscopic set-up has been described before (Palke et al. 2015). In brief, ^{57}Fe Mössbauer transmission spectra were recorded with a horizontal arrangement using a ^{57}Co/Rh single-line source with constant acceleration and a symmetric sawtooth velocity shape. The absorption data were collected with a multi-channel analyzer having 1024 channels and the velocity calibration was made using a 30 μm thick α-Fe foil. The FWHM associated with the ^{57}Co source is 0.243 ± 0.015. A powdered sample was contained in a plastic disc held a Cu-ring of 10 mm inner diameter, covered with high-purity Al-foil on the backside. The folded spectrum was evaluated by using Lorentzian-shaped doublets using the program RECOIL.

$C_p(T)$ was measured three times at 60 different temperature increments from 300 down to 2 K. The mass of the polycrystalline fayalite sample was 15.47 mg. The mass of the forsterite crystal platelet was 30.57 mg. The Quantum Design relaxation calorimeter and the experimental set-up used to measure C_p have been described before (Dachs and Bertoldi 2005; Geiger and Dachs 2018) and are not repeated here. Measurements on standard Al_2O_3 and/or MgO single crystals (Geiger and Dachs 2018) are made on a regular basis to check the experimental accuracy.

RESULTS

The X-ray results show that both samples are primarily olivine with only minor amounts of other phases (Supplementary Fig. 1a and Fig. 1b). The ^{57}Fe Mössbauer spectra are shown in Fig. 1a and 1b and they can be fitted well with two Fe^{2+} doublets. The fit parameters are given in Table 3. The amount of Fe^{3+} in both samples is very minor based on the minimal to nil absorption between 0.0 and 1.0 mm/s. No attempt was made to account for possible differences in the recoil-free fraction for Fe^{2+} at M1 and M2.

145 The $C_p(T)$ data from the relaxation-calorimetry measurements of the two natural olivines
146 are compared with the C_p behavior of synthetic olivines of similar compositions in Fig. 2a and
147 Fig. 2b. The data for the former samples are average values obtained from three separate C_p(2-
148 300 K) measurements (cf. raw data in Supplementary Tables 1a and 1b and one sigma errors).
149 The data for the two different synthetic fayalite samples are the smoothed values given in Robie
150 et al. (1982b) and Dachs et al. (2007). A pronounced paramagnetic-antiferromagnetic magnetic
151 transition and a Schottky anomaly, both related to Fe^{2+}, are apparent in the data of the fayalites.
152 The Néel temperature, T_N, of the magnetic transition is 64.9 K (Robie et al. 1982b) or 64.5 K
153 (Dachs et al. 2009) for synthetic fayalite and 63.1 K for the natural Rockport sample. A weak
154 and broad Schottky anomaly, arising from the spin-orbit interaction for Fe^{2+}, is centered at about
155 19 K for both types of crystals (Fig. 2a). The $S°$ value calculated (eqn. 2) for the Rockport
156 sample is 151.6 ± 1.1 J/mol·K ($S°$ is taken to be equal to $S^{calorimetric}$ at 298.15 K and the entropy
157 contribution for the temperature region between 0 and 2 K is negligible being about 0.003
158 J/mol·K). Uncertainties in $S°$ associated with relaxation calorimetry are discussed in Geiger and
159 Dachs (2018 - Table 1). The $S°$ value for Rockport olivine is indistinguishable from the values
160 obtained for synthetic fayalite of 151.0 ± 0.2 J/mol·K (Robie et al. 1982b) and 151.4 ± 0.1
161 J/mol·K (Dachs et al. 2009).
162 Figure 2b shows the C_p(2-300 K) results for the natural forsterite of composition
163 $Fo_{0.904}Fa_{0.096}$ and a synthetic olivine of comparable composition of $Fo_{0.90}Fa_{0.10}$ (Dachs et al.
164 2009). The intensity of the magnetic phase transition (i.e., magnon contribution to C_p) and T_N
165 decrease with decreasing Fe^{2+} in olivine (Dachs et al. 2009; Geiger et al. 2019). For this
166 forsterite-rich olivine, the C_p data show a weak and broad feature that is centered roughly at 20 K
167 and that probably is magnetic in nature. A very weak possible Schottky anomaly is centered at
168 about 13 K. Both can only be resolved, and separated from the vibrational (phonon) C_p, by
169 model calculations (Dachs et al. 2009). $S°$ for this synthetic $Fo_{0.90}Fa_{0.10}$ sample is 99.5 J/mol·K

(Dachs et al. 2009) and for the natural crystal we calculate 99.1 ± 0.7 J/mol·K (this includes 0.03 J/mol·K for the temperature region between 0 and 2 K).

DISCUSSION

Natural vs synthetic crystals

Olivine can be synthesized in the laboratory without the use of a flux and from high-purity component oxides. The experiment involves relatively short sintering times at high temperature (e.g. $T > 1000$ °C). For Fe^{2+}- bearing crystals the f_{O_2} conditions must be controlled. The resulting crystals are typically fine grained, roughly 1 to 100 micrometers in site. In nature, on the other hand, crystals can grow at lower temperatures (e.g. metamorphic regimes) and they do so over geologic time periods. They can be coarse grained ranging up to centimeters in size (of course, natural crystals can have varying modes of origin). Consequently, differences in structural state, that is Fe^{2+}-Mg order-disorder over the M1 and M2 sites, between synthetic and natural olivines can occur because of the different crystallization processes. Natural crystals from metamorphic or plutonic settings can, in general, be more ordered in terms of atomic structure compared to their synthetic analogues. Ordered crystals typically have stronger chemical bonding than disordered ones of the same composition. It follows that $C_p(T)$ and $S°$ values for the former should be smaller than the latter. Heat capacity and entropy effects related to long-range cation order-disorder in Fe^{2+}-Mg olivine solid solutions have not been investigated in a quantitative manner.

Natural olivine is expected to generally contain higher concentrations of minor or trace elements compared to synthetic crystals prepared from high purity reactants. Finally, there is also the issue of defect chemistry and point defects to consider and, here, there could also possibly be differences between synthetic and natural crystals. Some natural olivines may contain a little Fe^{3+} (Ejima et al. 2012), and minor structural OH^- can be present as well (Miller et al. 1987). What do the results of our X-ray, ^{57}Fe Mössbauer and C_p measurements show?

196

197 **X-ray diffraction and ^{57}Fe Mössbauer spectroscopic interpretation**

198 The X-ray results indicate that both olivine samples are nearly pure. Only small amounts
199 (about < 1 %) of other phases could be identified. The olivine diffraction peaks are intense and
200 narrow in width indicating good crystallinity (Supplementary Fig. 1). The ^{57}Fe Mössbauer
201 spectra can be fit well with two Fe^{2+} quadrupole-split doublets (Bancroft et al. 1967; Dyar et al.
202 2009). The amount of Fe^{3+} in both samples is very minor based on the minimal to nil absorption
203 between about 0.0 and 1.0 mm/sec (Fig. 1).

204 In terms of high-spin Fe^{2+} in olivine and for a first-order analysis, the magnitude of the
205 quadrupole splitting gives a measure of the asymmetry of the charge distribution around the Fe
206 nucleus (i.e., octahedral M-site distortion). It consists of valence and lattice terms, whereby the
207 latter decreases with increasing distortion. The isomer shift measures the *s* electron contact
208 density at the Fe nucleus (i.e., is a function of the ligand coordination). Diffraction results on
209 olivine indicate that M1 is smaller in volume and more distorted than M2 at room temperature
210 (Princivalle 1990). The assignments of the two Fe^{2+} doublets in Table 3 follow this reasoning.
211 The areas of the two doublets are similar. For the fayalite, the areas should be similar (assuming
212 that the small amount of Mn^{2+} in the olivine is not located largely at either M1 or M2). The
213 spectrum of the forsterite sample may show a slight tendency for Fe^{2+} to favor M2, but the
214 difference in doublet areas is within experimental error. The hyperfine parameters of both natural
215 olivines (Table 3) are in good agreement with those obtained on synthetic samples of similar
216 composition (Dyar et al. 2009), except possibly for the quadrupole split value for doublet 2 for
217 our fayalite (i.e., 2.71 mm/s) versus that of an end-member composition synthetic fayalite (i.e.,
218 2.76 mm/s).

219 A possible systematic difference between the spectra of natural and synthetic olivines
220 may lie in the values of the absorption line widths (i.e., FWHM). For the two natural crystals
221 they are the same with values of 0.24 mm/sec, whereas synthetics give values of about 0.29

222 mm/s for Fa_{100} and 0.27 mm/s for $Fo_{90}Fa_{10}$ (Dyar et al. 2009) A precise crystal-chemical
223 interpretation of the line widths is difficult to make, but larger widths may reflect more nearest
224 or next-nearest neighbor atomic disorder (i.e., structural heterogeneity).
225
226 **$C_p(T)$ and $S°$ behavior**
227 The C_p(2-300 K) behavior of natural fayalite and synthetic Fa_{100} is in excellent
228 agreement. Even C_p arising from magnon contributions and the Schottky anomaly is the same for
229 the two crystal types. This agreement is a rather remarkable result, we think, considering the
230 very different origins of the two olivine samples. There is a slight difference of about 2 K
231 between the T_N values (~65 K for synthetic samples vs 63 K for the natural crystal). In the case
232 of "end-member composition" silicate garnets, small variations in T_N can arise from minor
233 concentrations of "impurity" cations occurring in solid solution (Geiger et al. 2019). This is
234 possibly the case here as well, because the natural fayalite contains some Mn^{2+} substituting for
235 Fe^{2+}. Because Mn^{2+} and Fe^{2+} have similar masses (54.94 and 55.85 amu, respectively) and ionic
236 radii in six-fold coordination (83 pm vs 78 pm), their vibrational (phonon) behavior in olivine
237 should be similar. There is excellent agreement among the $S°$ values for synthetic fayalite of
238 151.0 ± 0.2 J/mol·K (Robie et al. 1982b) and 151.4 ± 0.1 J/mol·K (Dachs et al. 2007) and for the
239 natural fayalite (151.6 ± 1.1 J/mol·K).
240 The $C_p(T)$ behavior of the natural forsterite $Fo_{0.894}Fa_{0.106}$ and the synthetic $Fo_{90}Fa_{10}$
241 sample (Dachs et al. 2009) are in excellent agreement between about 7 and 300 K. It would
242 appear that any phonon differences arising from possible variations in Fe^{2+}-Mg order-disorder
243 are minimal to nil. The only observable differences in C_p behavior lie at $T < 7$ K. The natural
244 crystal does not show Debye T^3 behavior, but instead a quasi-plateauing of C_p between about 2
245 and 7 K (Fig. 2b). A physical interpretation for this result is difficult to make. There is very little
246 research, of any type, on silicates at such low temperatures. Many older adiabatic calorimetry
247 investigations were only made down to roughly 8 K. However, one could speculate that the

248 plateauing is due to an "impurity" atom such as Fe^{3+}. Gmelin (1969) showed in very low C_p
249 measurements down to 0.5 K on MgO that 340 ppm Fe^{3+} gives rise to an anomaly centered at
250 roughly 1-2 K. Such concentrations of Fe^{3+} in natural olivine are possible, but more work is
251 required to fully explain the nature of this C_p anomaly. This very low-temperature behavior is
252 not of great significance for chemical thermodynamic calculations but rather for its thermal
253 physical nature. The $S°$ of the crystal is 99.1 ± 0.7 J/mol·K and, thus, the same as that measured
254 for synthetic $Fo_{0.90}Fa_{0.10}$ having a value of 99.5 ± 0.1 J/mol·K (Dachs et al. 2007).
255
256 **IMPLICATIONS**
257 This work shows that there are no significant $C_p(T)$ differences in a chemical
258 thermodynamic sense between two selected natural olivine samples and their synthetic
259 equivalents, despite their contrasting crystallization histories and small differences in chemistry.
260 Further $C_p(T)$ measurements on additional intermediate olivine compositions are required to get
261 a more complete handle on any possible thermodynamic differences between both types of
262 phases. In addition, calorimetric measurements to determine enthalpies of formation and mixing
263 could be useful as well. ΔC_p(298 K) mixing behavior for olivines across the forsterite-fayalite
264 join, calculated from IR spectra, may be nonideal according to Hofmeister and Pitman (2007).
265 For silicates, most low-temperature calorimetric studies have concentrated on end-member
266 compositions in the case of substitutional-solid-solution systems. Moreover, older calorimetric
267 work was sometimes done on minerals that were not always well characterized structurally (e.g.,
268 structural state) and sometimes even compositionally. For these reasons, $C_p(T)$ and $S°$ behavior
269 for various silicate solid solutions and phases showing atomic order-disorder are, in general, still
270 not fully understood.
271

ACKNOWLEDGMENTS

We thank Dr. P. Pohwat of the Department of Mineral Sciences of the Smithsonian Institute, Washington D.C., USA, for supplying the fayalite sample (NMNH R 3517 00) and Dr. E. Ferré (University of Louisiana at Lafayette) for the forsterite crystal (NFo90/C1). G. Tippelt (Salzburg) kindly undertook the X-ray and Mössbauer measurements. This research was supported by a grant to C.A.G. from the Austrian Science Fund (FWF: P 30977-NBL). He also thanks the "Land Salzburg" for financial support through the initiative "Wissenschafts- und Innovationsstrategie Salzburg 2025".

280 **REFERENCES**

281

282 Bancroft, G.M., Maddock, A.G., and Burns, R.G. (1967) Applications of the Mössbauer effect to
283 silicate mineralogy – I. Iron silicates of known crystal structure. Geochimica et
284 Cosmochimica Acta, 31, 2219-2246.

285 Belley, F. et al. (2009) The magnetic properties of natural and synthetic $(Mg_{1-x}Fe^{2+}_x)_2SiO_4$
286 olivines. Earth and Planetary Sciences Letters, 284, 516-526.

287 Cloutis, E.A. (2015) Mineral and rock sample database. Planetary Spectrophotometer Facility
288 (PSF), University of Winnipeg. 1-1026. https://ctape.uwinnipeg.ca/Samples_Directory/

289 Dachs, E. and Bertoldi, C. (2005) Precision and accuracy of the heat-pulse calorimetric
290 technique: low-temperature heat capacities of milligram-sized synthetic mineral samples.
291 European Journal of Mineralogy, 17, 251-261.

292 Dachs, E., Geiger, C.A., Benisek, A., and Grevel, K-D. (2012) Grossular: A crystal-chemical,
293 calorimetric, and thermodynamic study. American Mineralogist, 97, 1299-1313.

294 Dachs, E., Geiger, C.A., von Seckendorff, V., and Grodzicki, M. (2007) A low-temperature
295 calorimetric study of synthetic (forsterite-fayalite) $\{(Mg_2SiO_4\text{-}Fe_2SiO_4)\}$ solid solutions:
296 An analysis of vibrational, magnetic and electronic contributions to the molar heat
297 capacity and entropy of mixing. Journal of Chemical Thermodynamics, 39, 906-933.

298 Dyar, M.D., Delaney, J.S., Sutton, S.R., and Schaefer, W. (1998) Fe^{3+} distribution in oxidized
299 olivine: A synchrotron micro-XANES study. American Mineralogist, 83, 1361-1365
300 (1998).

301 Dyar, M.D. et al. (2009) Spectroscopic characteristics of synthetic olivine: An integrated multi-
302 wavelength and multi-techniques approach. American Mineralogist, 94, 883-898.

303 Ejima, T., Akasaka, M., Nago, T., and Ohfuji, H. (2012) Oxidation state of Fe in olivine in
304 andesitic scoria from Kasayama volcano, Hagi, Yamaguchi Prefecture, Japan. Journal of
305 Mineralogical and Petrological Sciences, 107, 215-222.

306 Geiger, C.A. and Dachs, E. (2018) Recent developments and the future of low-*T* calorimetric
307 investigations in the Earth sciences: Consequences for thermodynamic calculations and
308 databases. Journal of Metamorphic Geology, 36, 283-295.
309 Geiger, C.A., Grodzicki, M., and Dachs, E. (2019) An analysis of the magnetic behavior of
310 olivine and garnet substitutional solid solutions. American Mineralogist, 104, 1246-1255.
311 Gmelin, E. (1969) Anomalies in the low temperature heat capacities of BeO and MgO,
312 containing Fe^{3+}. Journal Physics and Chemistry of Solids, 30, 2789-2792.
313 Harlow, G. and Thu, K. (2014) Peridot from Pyaung-gaung, Mogok Tract, Myanmar:
314 Similarities to Sapat and Zabargad deposits. Twelfth Annual Sinkakas Symposium
315 – Peridot and Uncommon Green Gem Minerals, 83-95.
316 Helgeson, H.C., Delany, J.M., Nesbitt, H.W., and Bird, D.K. (1978) Summary and critique of the
317 thermodynamic properties of rock-forming minerals. American Journal of Science, 278-
318 A, 1-229.
319 Hofmeister, A.M. and Pitman, K.M. (2007) Evidence for kinks in structural and thermodynamic
320 properties across the forsterite-fayalite binary from thin-film IR absorption spectra.
321 Physics and Chemistry of Minerals, 34, 319-333.
322 Keleman, P.B. et al. (2011) Rates and mechanisms of mineral carbonation in peridotite: Natural
323 processes and recipes for enhanced, in situ CO_2 capture and storage. Annual Reviews of
324 Earth and Planetary Sciences, 39, 545-576.
325 Miller, G.H., Rossman, G.R., and Harlow, G.E. (1987) The natural occurrence of hydroxide in
326 olivine. Physics and Chemistry of Minerals, 14, 461-472.
327 Palke, A.C., Stebbins, J.F., Geiger, C.A., and Tippelt, G. (2015) Cation order-disorder in Fe-
328 bearing pyrope and grossular garnets: An ^{27}Al and ^{29}Si MAS NMR and ^{57}Fe Mössbauer
329 spectroscopy study. American Mineralogist, 100, 536-547.
330 Palache, C. (1950) Fayalite at Rockport, Massachusetts. American Mineralogist, 35, 877-881.
331 Princivalle, F. (1990) Influence of temperature and composition on Mg-Fe^{2+} intracrystalline
332 distribution in olivines. Mineralogy and Petrology, 43, 121-129.

Rose, T.R., Sorensen, S.S., and Post, J.E. (2009) The impurities in the Rockport fayalite microbeam standard: How bad are they? American Geophysical Union, abstract id. V31E-2008.

Robie, R.A. and Hemingway B.S. (1995) Thermodynamic properties of minerals and related substances at 298.15 K and 1 bar (10^5 pascals) pressure and at higher temperatures. 461 p. United States Geological Survey Bulletin, Washington D.C. 2131.

Robie, R.A., Hemingway, B.S., and Takei, H. (1982a) Heat capacities and entropies of Mg_2SiO_4, Mn_2SiO_4, and Co_2SiO_4 between 5 and 380 K. American Mineralogist, 67, 470-482.

Robie, R.A., Finch, C.B, and Hemingway, B.S. (1982b) Heat capacity and entropy of fayalite (Fe_2SiO_4) between 5.1 and 383 K: comparison of calorimetric and equilibrium values for the QFM buffer reaction. American Mineralogist, 67, 463-469.

Westrum, E.F. Jr. (1962) Cryogenic calorimetric contributions to chemical thermodynamics. Journal of Chemical Education, 39, 443-454.

Figure Captions

Figure 1. ^{57}Fe Mössbauer spectra of natural olivine samples. (a) NMNH R3517 fayalite from Rockport, MA, USA and (b) C1/NFo90 forsterite from Mogok, Myanmar. The spectra are fitted with two different symmetric quadrupole split doublets. The green doublet with the larger quadrupole split value corresponds to Fe^{2+} at the octahedrally coordinated M2 site and the red doublet with the smaller value to Fe^{2+} at M1 (see Table 3).

Figure 2. C_p data from 2 to 300 K. (a) The brown circles are data for nearly end-member fayalite NMNH R3517 from Rockport, MA, USA, the "x" symbols (Dachs et al. 2007) and the "+" symbols (Robie et al. 1982b) for synthetic fayalite. The inset shows the lowest temperature region and note the Schottky anomaly. (b) The green circles are data for the natural forsterite, $Fo_{0.904}Fa_{0.096}$, from the Pyaung-gaung Mine, Mogok, Katha District, Myanmar and the "+" symbols for synthetic $Fo_{90}Fa_{10}$ (Dachs et al. 2007). The inset shows the lowest temperature region and note the plateauing of C_p values below about 7 K.

375 Figure 1.

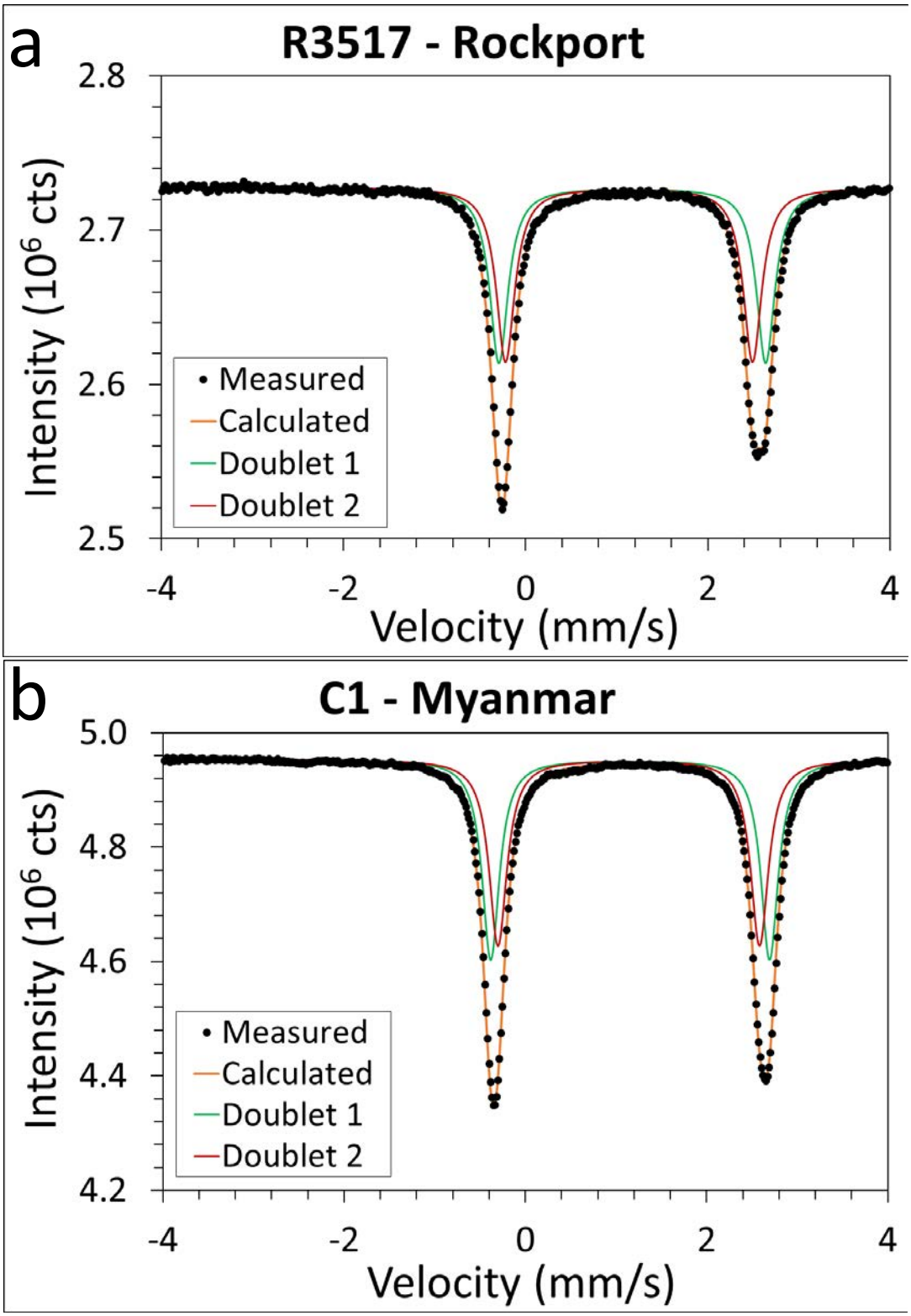

376

377

378

379

380 Figure 2a

381

382

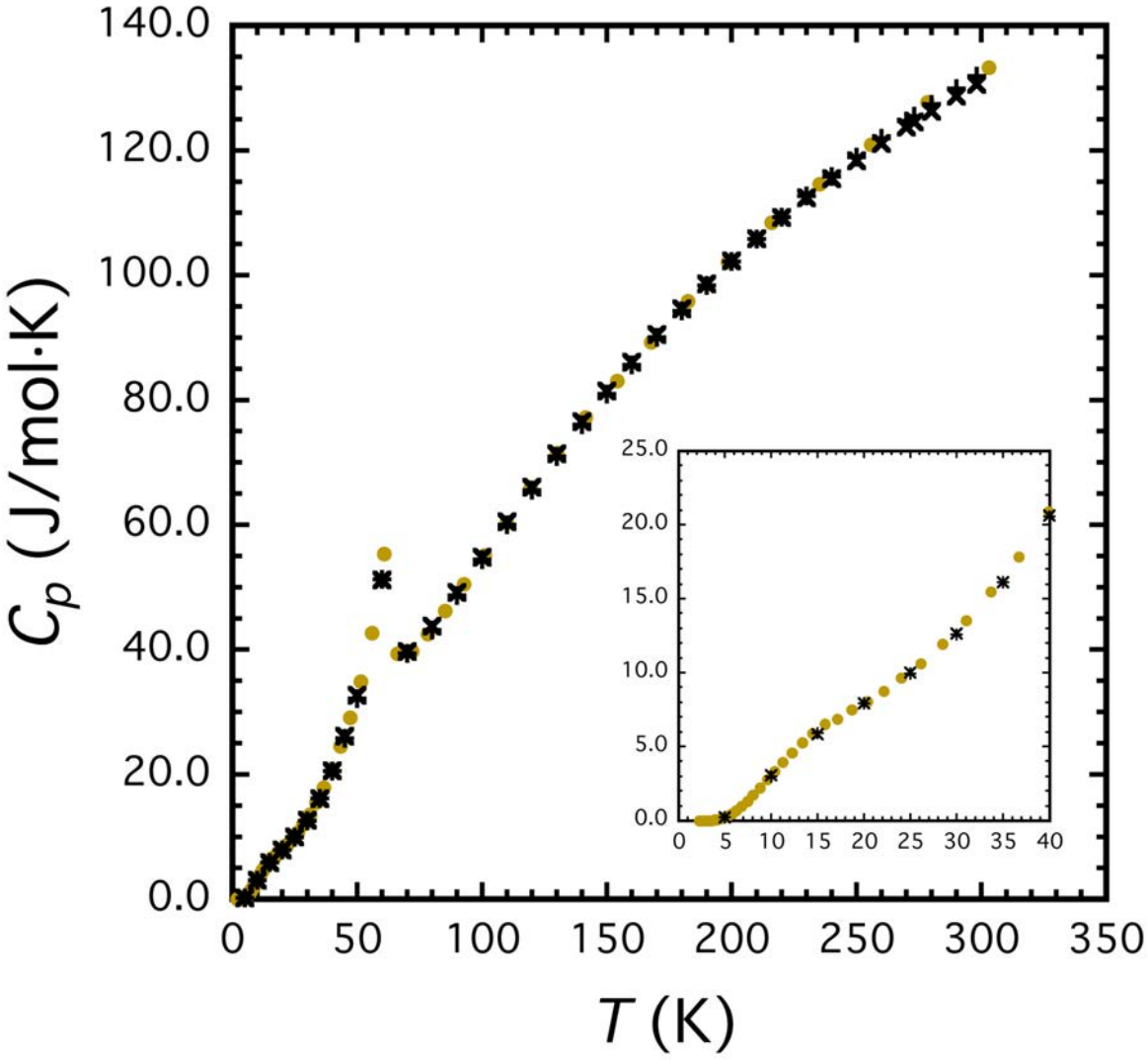

383

384

385

386

Figure 2b

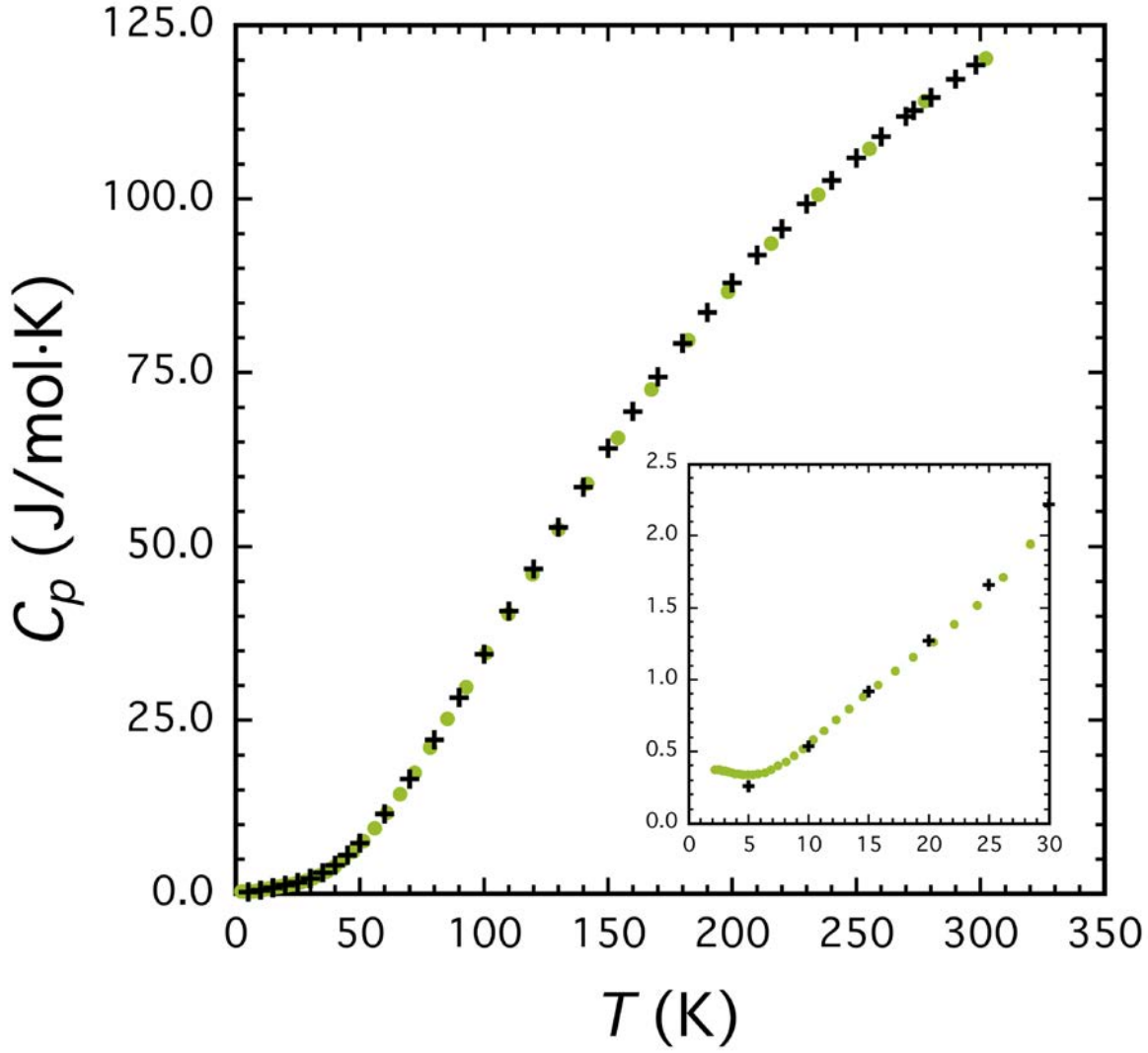

Table 1. Olivines used for investigation.

Label	Locality (Source)	Sample Description and References
NFo90/C1	Pyaung-gaung Mine, Mogok, Katha District, Myanmar (E. Ferré)	~5 mm size gemmy-like crystals within metamorphosed dolomitic limestone[1,2]
NMNH R 3517 00	Rockport, Massachusetts, USA (Smithsonian Institute)	Isolated fayalite-rich rock masses in pegmatite and granite; xenolithic[3,4,5,6]

[1] Belley et al. (2009), [2] Harlow and Thu (2014), [3]Palache (1950), [4]Dyar et al. (1998), [5]Rose et al. (2015), [6]Cloutis et al. (2015)

Table 2. Published microprobe results for the two studied olivine samples in oxide wt. % and the calculated crystal-chemical formulae based on four oxygens.

Sample	NMNH R3517[1]	NFo90/C1[2]
SiO_2	29.78	40.9
FeO	66.48	9.4
MgO	0.05	49.4
MnO	2.14	-
ZnO	0.54	-
NiO/Ni_2O_3	0.04	0.3
CaO	0.05	-
TiO_2	Trace	-
CoO	0.10	-
Total	99.18	100.0
Si	1.01	1.00
Fe^{2+}	1.89	0.19
Mg	-	1.80
Mn^{2+}	0.06	-
Zn^{2+}	-	-
Ni	-	0.01
Total	2.96	3.00

[1]Cloutis et al. (2015) and [2]Belley et al. (2009).

Table 3. Fit parameters for the ^{57}Fe Mössbauer spectra. Two Fe^{2+} quadrupole split doublets were fit to the spectra of both olivine samples.

Sample	Doublet 1 - Fe^{2+} at M2				Doublet 2 - Fe^{2+} at M1				χ^2
	Δ mm/s	δ mm/s	Γ mm/s	Area %	Δ mm/s	δ mm/s	Γ mm/s	Area %	
Fayalite NMNH R3517	2.93	1.17	0.24	50.0	2.71	1.13	0.24	50.0	1.17
Forsterite NFo90/C1	3.08	1.15	0.24	50.9	2.89	1.14	0.24	49.1	1.94

The parameters for Δ (quadrupole splitting), δ (isomer shift relative to α-Fe foil) and Γ (FWHM) are given to the second decimal and one decimal for the areas. Errors in the former are less than ± 0.02 mm/s, whereas for the areas they are less than about ± 5%.

Geiger et al. (2020) Are the Thermodynamic Properties of Natural and Synthetic Olivines the Same?

Supplementary Figure 1a. XRD pattern for Rockport natural olivine sample NMNH R3517 from Rockport, MA, USA.

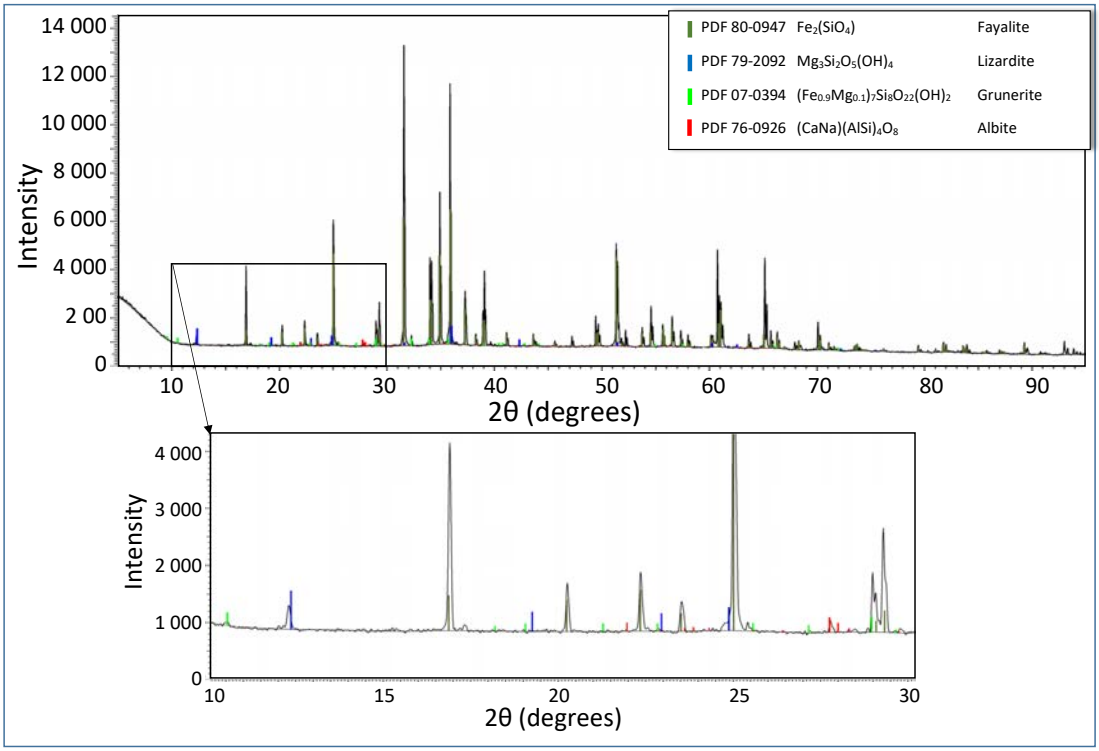

Supplementary Fig. 1a

Geiger et al. (2020) Are the Thermodynamic Properties of Natural and Synthetic Olivines the Same?

Supplementary Figure 1b. XRD pattern for natural olivine sample C1/NFo90 from Mogok, Myanmar.

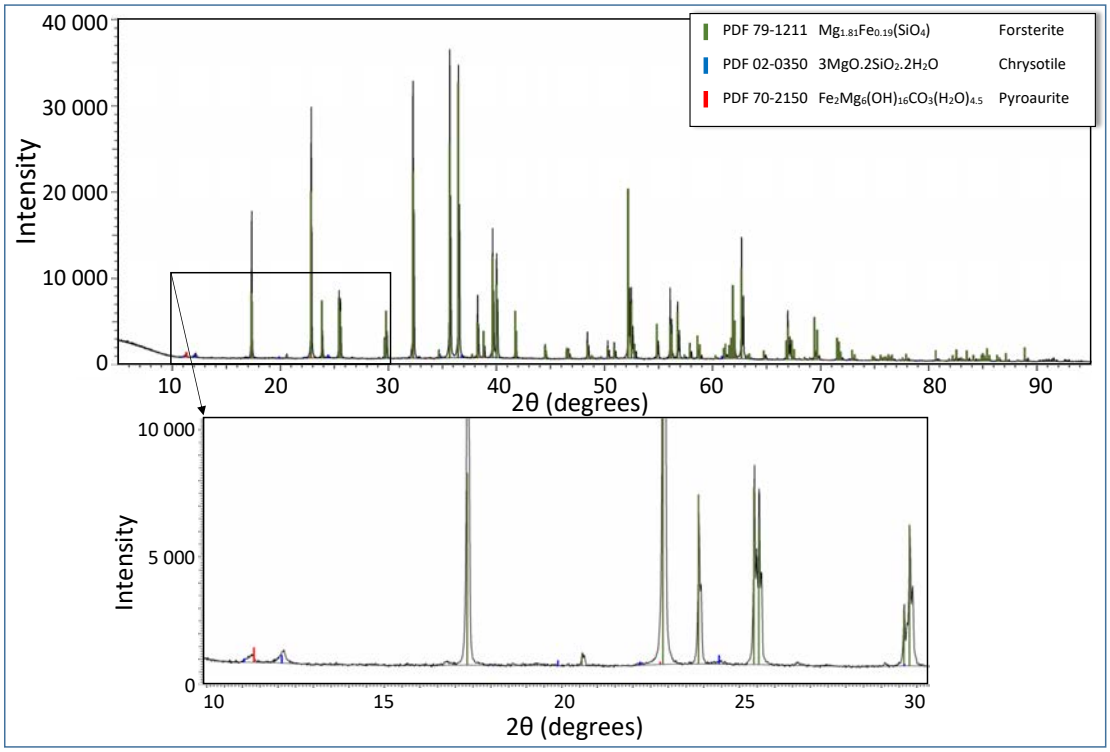

Supplementary Fig. 1b

Geiger et al. (2020) Are the Thermodynamic Properties of Natural and Synthetic Olivines the Same?

Supplementary Table 1a: PPMS Data

Natural Olivine Sample NMNH R-3517 from Rockport, MA, USA

Formula Weight 203.199 g/mol

Sample Weight 15.47 mg

PPMS-1			PPMS-2			PPMS-3		
T (K)	Cp (J/mol.K)	1 sigma (J/mol.K)	T (K)	Cp (J/mol.K)	1 sigma (J/mol.K)	T (K)	Cp (J/mol.K)	1 sigma (J/mol.K)
2.20	0.0068	0.0002	2.20	0.0068	0.0002	2.20	0.0068	0.0002
2.38	0.0080	0.0002	2.38	0.0080	0.0002	2.38	0.0081	0.0002
2.58	0.0097	0.0002	2.58	0.0097	0.0002	2.58	0.0098	0.0002
2.79	0.0123	0.0003	2.79	0.0123	0.0003	2.80	0.0124	0.0003
3.02	0.0167	0.0004	3.02	0.0166	0.0004	3.03	0.0169	0.0004
3.27	0.0241	0.0005	3.27	0.0241	0.0005	3.28	0.0242	0.0004
3.54	0.0366	0.0006	3.54	0.0366	0.0006	3.56	0.0376	0.0007
3.84	0.0579	0.0009	3.84	0.0583	0.0001	3.85	0.0588	0.0009
4.16	0.0926	0.0012	4.16	0.0929	0.0012	4.16	0.0930	0.0012
4.51	0.1471	0.0019	4.51	0.1475	0.0019	4.52	0.1486	0.0017
4.89	0.2281	0.0027	4.89	0.2284	0.0027	4.90	0.2299	0.0024
5.31	0.3439	0.0036	5.31	0.3447	0.0039	5.32	0.3457	0.0033
5.77	0.5062	0.0051	5.78	0.5070	0.0055	5.78	0.5074	0.0044
6.27	0.7208	0.0072	6.28	0.7225	0.0072	6.28	0.7177	0.0059
6.82	1.0004	0.0098	6.82	0.9989	0.0096	6.83	0.9987	0.0085
7.41	1.3344	0.0114	7.41	1.3392	0.0131	7.41	1.3382	0.0129
8.05	1.7392	0.0154	8.05	1.7429	0.0170	8.06	1.7422	0.0169
8.76	2.2158	0.0200	8.76	2.2215	0.0217	8.76	2.2224	0.0217
9.52	2.7615	0.0258	9.53	2.7608	0.0268	9.53	2.7601	0.0266
10.36	3.3500	0.0324	10.36	3.3548	0.0319	10.36	3.3542	0.0319
11.26	3.9786	0.0389	11.26	3.9749	0.0392	11.27	3.9776	0.0384
12.25	4.6135	0.0462	12.25	4.6138	0.0451	12.25	4.6196	0.0452
13.32	5.2579	0.0529	13.32	5.2562	0.0524	13.32	5.2573	0.0527
14.48	5.8798	0.0598	14.49	5.9095	0.0610	14.50	5.8737	0.0587
15.74	6.5071	0.0670	15.76	6.5207	0.0675	15.78	6.4785	0.0574
17.14	6.9134	0.0114	17.16	6.9102	0.0128	17.17	6.7812	0.0132
18.62	7.4938	0.0122	18.64	7.5036	0.0143	18.68	7.5259	0.0635
20.30	8.1667	0.0173	20.30	8.2270	0.0271	20.32	7.8208	0.0382
22.07	8.9081	0.0196	22.07	8.8544	0.0173	22.12	8.5896	0.0420
24.02	9.6664	0.0163	24.03	9.6696	0.0162	24.04	9.5823	0.0190
26.13	10.6953	0.0188	26.15	10.6894	0.0186	26.15	10.6029	0.0318
28.44	11.9478	0.0216	28.44	11.9868	0.0426	28.45	11.9561	0.0219
30.95	13.4968	0.0265	30.95	13.5651	0.0375	30.95	13.5059	0.0262
33.67	15.4585	0.0314	33.67	15.6108	0.0496	33.68	15.4695	0.0310
36.64	17.8513	0.0376	36.65	17.9522	0.0526	36.65	17.8434	0.0381
39.87	20.8453	0.0443	39.88	20.8375	0.0450	39.88	20.9730	0.0667
43.38	24.4836	0.0534	43.39	24.4936	0.0539	43.40	24.6192	0.0805
47.20	29.0521	0.0639	47.20	29.0571	0.0644	47.24	29.0730	0.0685
51.36	34.8574	0.0782	51.36	34.8503	0.0793	51.41	34.8735	0.0814
55.89	42.6333	0.1011	55.89	42.6257	0.1014	55.96	42.7261	0.1050
60.74	55.1386	0.1802	60.82	55.4469	0.1598	60.83	55.4948	0.1621
66.15	39.6367	0.0897	66.17	39.2105	0.0694	66.19	39.2024	0.0708
72.01	39.9202	0.0927	72.02	39.6035	0.0844	72.03	39.6440	0.0900
78.36	42.4239	0.0941	78.36	42.6452	0.0983	78.38	42.4516	0.0919
85.26	46.6527	0.1250	85.28	46.0886	0.1400	85.30	45.8705	0.1124
92.78	50.3582	0.1149	92.78	50.7406	0.1242	92.79	50.2828	0.1105
100.95	55.0453	0.1216	100.96	54.9349	0.1332	100.96	55.3364	0.1315
109.86	60.1981	0.1551	109.86	60.2876	0.1319	109.87	60.5970	0.1655
119.52	66.1514	0.1697	119.55	66.1321	0.1568	119.56	65.6792	0.1466
130.07	71.6593	0.1634	130.09	71.4437	0.1591	130.09	71.4813	0.1597
141.58	77.2592	0.1710	141.58	77.2863	0.1680	141.59	77.0910	0.1624
154.05	83.0177	0.1707	154.07	83.1261	0.1763	154.10	82.9307	0.1685
167.66	89.3509	0.1988	167.67	89.2028	0.1863	167.70	89.3459	0.1801
182.47	95.8952	0.2188	182.48	95.8418	0.1968	182.51	95.7908	0.1978
198.56	102.1175	0.2127	198.57	102.1106	0.2033	198.58	102.1659	0.2096
216.05	108.5412	0.2241	216.09	108.4266	0.2132	216.10	108.2839	0.2178
235.08	114.6084	0.2075	235.16	114.6105	0.2192	235.17	114.5771	0.2254
255.81	120.8214	0.2208	255.92	120.9454	0.2274	255.92	120.9204	0.2361
278.35	127.8001	0.2539	278.49	127.6240	0.2634	278.50	127.7032	0.2648
302.92	133.1141	0.2400	303.04	133.2912	0.2532	303.05	133.3933	0.2580

Geiger et al. (2020) Are the Thermodynamic Properties of Natural and Synthetic Olivines the Same?

Supplementary Table 1b: PPMS Data

Natural Olivine Sample C1/NFo90 from Mogok, Myanmar

Formula Weight 146.441 g/mol

Sample Weight 30.57 mg

PPMS-1			PPMS-2			PPMS-3		
T (K)	Cp (J/mol.K)	1 sigma (J/mol.K)	T (K)	Cp (J/mol.K)	1 sigma (J/mol.K)	T (K)	Cp (J/mol.K)	1 sigma (J/mol.K)
2.20	0.3741	0.0010	2.22	0.3746	0.0011	2.22	0.3745	0.0011
2.38	0.3764	0.0009	2.39	0.3763	0.0010	2.39	0.3763	0.0010
2.57	0.3747	0.0008	2.59	0.3744	0.0009	2.59	0.3744	0.0009
2.78	0.3703	0.0007	2.80	0.3700	0.0008	2.80	0.3700	0.0008
3.02	0.3654	0.0007	3.03	0.3649	0.0007	3.03	0.3649	0.0007
3.27	0.3618	0.0008	3.29	0.3601	0.0007	3.29	0.3601	0.0007
3.54	0.3557	0.0007	3.56	0.3554	0.0007	3.56	0.3553	0.0006
3.84	0.3505	0.0006	3.86	0.3504	0.0006	3.86	0.3502	0.0006
4.16	0.3453	0.0006	4.18	0.3449	0.0006	4.18	0.3449	0.0006
4.51	0.3413	0.0006	4.53	0.3407	0.0005	4.53	0.3407	0.0005
4.90	0.3387	0.0006	4.91	0.3390	0.0005	4.92	0.3389	0.0005
5.32	0.3411	0.0006	5.33	0.3411	0.0005	5.33	0.3408	0.0005
5.78	0.3465	0.0006	5.79	0.3454	0.0004	5.79	0.3454	0.0004
6.29	0.3569	0.0006	6.30	0.3566	0.0004	6.31	0.3514	0.0008
6.84	0.3755	0.0005	6.85	0.3759	0.0005	6.85	0.3757	0.0005
7.40	0.3995	0.0006	7.42	0.3998	0.0006	7.42	0.4000	0.0005
8.05	0.4321	0.0007	8.06	0.4324	0.0006	8.07	0.4326	0.0006
8.75	0.4720	0.0008	8.76	0.4726	0.0007	8.77	0.4725	0.0007
9.52	0.5226	0.0009	9.53	0.5226	0.0007	9.53	0.5225	0.0008
10.35	0.5801	0.0010	10.36	0.5813	0.0009	10.37	0.5812	0.0008
11.26	0.6471	0.0011	11.28	0.6476	0.0010	11.28	0.6480	0.0009
12.25	0.7193	0.0013	12.27	0.7200	0.0011	12.27	0.7199	0.0010
13.33	0.7973	0.0014	13.34	0.7964	0.0011	13.34	0.7975	0.0011
14.49	0.8811	0.0015	14.51	0.8834	0.0013	14.51	0.8803	0.0011
15.76	0.9693	0.0017	15.77	0.9681	0.0012	15.78	0.9692	0.0012
17.15	1.0602	0.0013	17.15	1.0622	0.0017	17.17	1.0612	0.0012
18.64	1.1589	0.0015	18.66	1.1601	0.0015	18.67	1.1667	0.0018
20.29	1.2672	0.0021	20.30	1.2656	0.0016	20.32	1.2565	0.0029
22.07	1.3857	0.0025	22.08	1.3957	0.0023	22.10	1.3819	0.0018
24.00	1.5319	0.0023	24.01	1.5319	0.0026	24.04	1.5068	0.0035
26.12	1.7124	0.0025	26.12	1.7350	0.0045	26.16	1.7032	0.0027
28.42	1.9476	0.0034	28.44	1.9501	0.0029	28.45	1.9293	0.0053
30.92	2.2617	0.0041	30.95	2.2647	0.0035	30.96	2.2374	0.0065
33.65	2.6820	0.0045	33.67	2.6831	0.0043	33.67	2.6685	0.0066
36.61	3.2347	0.0054	36.63	3.2205	0.0080	36.63	3.2356	0.0052
39.84	3.9760	0.0082	39.84	3.9709	0.0070	39.86	3.9699	0.0067
43.36	4.9101	0.0080	43.36	4.9457	0.0093	43.37	4.9144	0.0079
47.18	6.1083	0.0101	47.18	6.1577	0.0119	47.19	6.1098	0.0098
51.33	7.6026	0.0125	51.34	7.6515	0.0136	51.34	7.6045	0.0120
55.85	9.4486	0.0150	55.86	9.5348	0.0187	55.87	9.4500	0.0147
60.77	11.6749	0.0181	60.78	11.7758	0.0222	60.79	11.6727	0.0175
66.13	14.3422	0.0216	66.14	14.4550	0.0267	66.15	14.3345	0.0212
71.96	17.4638	0.0248	71.98	17.5456	0.0290	71.98	17.4479	0.0240
78.29	21.0272	0.0288	78.30	21.0562	0.0333	78.32	21.2053	0.0380
85.19	25.2178	0.0355	85.20	25.1929	0.0351	85.21	25.3134	0.0406
92.71	29.6847	0.0446	92.71	29.7228	0.0417	92.73	29.9075	0.0516
100.86	34.6914	0.0418	100.88	34.6930	0.0475	100.89	34.8604	0.0474
109.77	40.1889	0.0503	109.77	40.3561	0.0519	109.80	40.4910	0.0638
119.44	46.1130	0.0525	119.46	46.0715	0.0534	119.46	46.0247	0.0695
129.98	52.3869	0.0580	129.98	52.4046	0.0607	129.98	52.4847	0.0666
141.46	58.9585	0.0647	141.46	59.1419	0.0857	141.47	58.9270	0.0649
153.91	65.7995	0.0726	153.93	65.4681	0.0701	153.93	65.5457	0.0721
167.41	72.6399	0.0770	167.41	72.5775	0.0713	167.46	72.5135	0.0754
182.14	79.7860	0.0871	182.15	79.5801	0.0782	182.20	79.5904	0.0807
198.18	86.6540	0.0858	198.19	86.5538	0.0786	198.20	86.6685	0.0824
215.63	93.6645	0.0874	215.65	93.5563	0.0868	215.65	93.6308	0.0864
234.56	100.6279	0.0943	234.61	100.6279	0.0921	234.62	100.5808	0.0918
255.16	107.2416	0.1031	255.25	107.2130	0.1002	255.26	107.2119	0.0953
277.56	114.1500	0.1285	277.70	114.1214	0.1239	277.71	114.0653	0.1095
302.11	120.2111	0.1116	302.12	120.3084	0.1062	302.13	120.1889	0.1071